BIOCHEMISTRY
including biophysical chemistry & molecular biology

ARTICLE

pubs.acs.org/biochemistry

Structural Instability and Cu-Dependent Pro-Oxidant Activity Acquired by the Apo Form of Mutant SOD1 Associated with Amyotrophic Lateral Sclerosis

Furi Kitamura, Nobuhiro Fujimaki, Wakana Okita, Hirotsugu Hiramatsu, and Hideo Takeuchi*

Graduate School of Pharmaceutical Sciences, Tohoku University, Aobayama, Sendai 980-8578, Japan

Supporting Information

ABSTRACT: Cu,Zn-superoxide dismutase (SOD1) is a cytosolic antioxidant enzyme, and its mutation has been implicated in amyotrophic lateral sclerosis (ALS), a disease causing a progressive loss of motor neurons. Although the pathogenic mechanism of ALS remains unclear, it is hypothesized that some toxic properties acquired by mutant SOD1 play a role in the development of ALS. We have examined the structural and catalytic properties of an ALS-linked mutant of human SOD1, His43Arg (H43R), which is characterized by rapid disease progression. As revealed by circular dichroism spectroscopy, H43R assumes a stable β-barrel structure in the Cu^{2+},Zn^{2+}-bound holo form, but its metal-depleted apo form is highly unstable and readily unfolds or misfolds into an irregular structure at physiological temperature. The conformational change occurs as a two-state transition from a nativelike apo form to a denatured apo form with a half-life of ~0.5 h. At the same time as the denaturation, the apo form of H43R acquires pro-oxidant potential, which is fully expressed in the presence of Cu^{2+} and H_2O_2, as monitored with a fluorogenic probe for detecting pro-oxidant activity. Comparison of d−d absorption bands suggests that the Cu^{2+} binding mode of the denatured apo form is different from that of the native holo form. The denatured apo form of H43R is likely to provide non-native Cu^{2+} binding sites where the Cu^{2+} ion is activated to catalyze harmful oxidation reactions. This study raises the possibility that the structural instability and the resultant Cu-dependent pro-oxidant activity of the apo form of mutant SOD1 may be one of the pathogenic mechanisms of ALS.

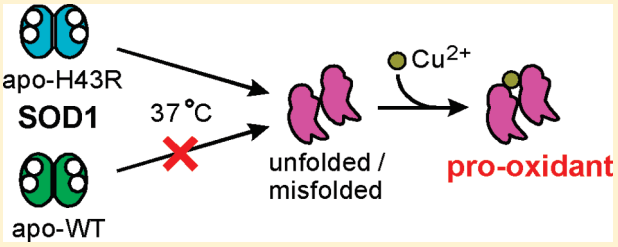

Amyotrophic lateral sclerosis (ALS) is a fatal neurodegenerative disease characterized by a progressive loss of motor neurons in the brain and spinal cord.[1] The pathogenesis of ALS is not well understood, and no effective therapeutic treatments have been established. Although ALS is mostly sporadic, the disease is inherited within families in 5−10% of all ALS cases.[2,3] Approximately 20% of such familial ALS patients have a variety of gene mutations of the cytosolic enzyme Cu,Zn-superoxide dismutase (SOD1).[3−7] Sporadic ALS is clinically and pathologically similar to familial ALS,[1] and gene mutations of SOD1 have also been found in 2−7% of the sporadic ALS patients.[1,8,9] Currently, the SOD1 mutation is most commonly associated with ALS, in particular with familial ALS.[7,10,11] Despite intensive biochemical and pathological studies, it is still unclear how mutant SOD1 is involved in the pathogenesis of ALS.

Wild-type SOD1 is a very stable and extremely efficient enzyme that catalyzes the dismutation of biologically toxic superoxide into less toxic hydrogen peroxide and molecular oxygen.[10,12,13] The polypeptide chain of human SOD1 consists of 153 amino acid residues, and two identical polypeptide chains compose a noncovalently linked dimer.[14,15] Each subunit of the dimeric protein is folded into a β-barrel structure and contains one Cu and one Zn ion in the catalytic site located on the outer surface of the β-barrel as shown in Figure 1.[16,17] In addition to the catalytic role, the active-site metal ions are reported to contribute to the stability of the dimeric β-barrel structure of SOD1.[13]

More than 140 mutations of SOD1 have so far been associated with ALS, and the ALS-linked mutations are scattered over approximately half of the total amino acid residues without distinct localization near the catalytic site (Figure 1) (ref 7 and http://alsod.iop.kcl.ac.uk/). Reflecting the variety of mutation points, some mutants completely lose dismutase activity, while others retain activity comparable to that of the wild-type protein.[7] Transgenic mice expressing dismutase-active mutants of human SOD1 show hallmarks of ALS pathology, whereas those expressing the dismutase-active wild type do not.[18,19] Accordingly, it is now considered that new toxic properties, but not the altered dismutase activity, of mutant SOD1 are associated with the pathogenesis of ALS.[7,18,19]

The mechanisms so far proposed for the gain of toxic properties by mutant SOD1 include the following two major hypotheses. (i) The mutation partly reduces the stability of protein structure, in particular in the metal-depleted apo form, and the structural instability gained by the mutant leads to the protein

Received: March 7, 2011
Revised: April 20, 2011
Published: April 20, 2011

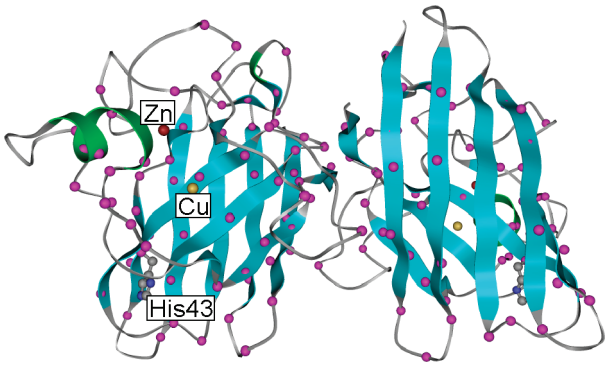

Figure 1. Dimeric β-barrel structure of human SOD1 in the holo form. Cu, Zn, and His43 are labeled in the left subunit. In the right subunit, they are hiding behind the β-barrel. The C_α atoms colored magenta indicate the locations of ALS-linked mutations. The α-helix, β-sheet, and irregular structure are colored green, sky blue, and gray, respectively. The atomic coordinates were taken from Protein Data Bank entry 1HL5, and the locations of ALS-linked mutations are from http://alsod.iop.kcl.ac.uk/.

unfolding and formation of cytotoxic aggregates.[20−23] (ii) The mutation modifies the active-site structure to catalyze new oxidative reactions, and the pro-oxidant activity gained by the mutant leads to a significant increase in the level of cellular oxidative stress.[24−28] These two hypotheses are currently being tested, in most cases as separate mechanisms, to elucidate the toxic role of mutant SOD1 in the pathogenesis of ALS.

In this study, we have investigated the possibility of the concomitant occurrence of structural instability and pro-oxidant activity by using an ALS-linked mutant of human SOD1, His43Arg (H43R), which is classified into a group of mutants that cause rapid progression of ALS.[7,29] His43 is one of the residues comprising the core of the β-barrel (Figure 1), and its imidazole side chain interacts with the hydrophobic "cork" (Leu38) that closes one end of the β-barrel.[17] Furthermore, His43 is hydrogen bonded with one of the Cu ligands,[16] implying a contribution to the catalytic activity.[30] Accordingly, the H43R mutation is expected to affect both structural and catalytic properties of the enzyme. Structural and biochemical analyses by circular dichroism (CD), visible−near-infrared absorption, and fluorometric assay have clearly shown that H43R gains a strong propensity to unfold or misfold into an irregular structure upon removal of the active-site Cu^{2+} and Zn^{2+} ions. The metal-depleted apo form of H43R acquires pro-oxidant activity when Cu^{2+} binds to non-native binding sites of the denatured structure, implying a toxic role of denatured, mismetalated SOD1 mutants in the development of ALS.

MATERIALS AND METHODS

Preparation of Recombinant Human SOD1 in the Holo Form. Recombinant human SOD1 was expressed in *Escherichia coli* cells harboring plasmid pET15b, which contained a human SOD1 cDNA fused with an N-terminal hexa-His tag.[31] A QuickChange site-directed mutagenesis kit (Stratagene) was used to create the H43R mutant. The resulting plasmid was sequenced to confirm the mutation. The gene-transformed *E. coli* cells were cultured in Luria-Bertani medium containing 50 μg/mL ampicilin at 37 °C and harvested by centrifugation, followed by sonication for cell disruption and by solubilization of the protein from inclusion bodies.[32] Isolation of His-tagged SOD1 from the supernatant of the cell lysate was performed by using an immobilized metal affinity chromatography (IMAC) column charged with Ni^{2+} (HisTrap HP, GE Healthcare). The His tag was proteolytically cleaved from the protein with thrombin, and the resultant His tag fragments were removed with the IMAC column. Cu^{2+} and Zn^{2+} ions were incorporated into the His tag-removed protein by dialysis against sodium acetate (pH 5.5) containing $(CH_3COO)_2Zn$ and $CuSO_4$.[33] A chelation assay using 4-pyridylazaresorcinol showed full metalation for both the wild type and mutant.[34] The protein in the Cu^{2+},Zn^{2+}-bound holo form (holo-SOD1) was purified on a gel filtration column (Sephacryl-100, GE Healthcare), dialyzed against deionized water, and then freeze-dried. The dried protein was stored at −80 °C. The identity and purity of the final products were analyzed by sodium dodecyl sulfate−polyacrylamide gel electrophoresis, activity gel electrophoresis, and a colorimetric dismutase activity assay.[35] More detailed procedures for expression, isolation, purification, and characterization of the recombinant SOD1 proteins in the holo form are given in the Supporting Information together with a figure (Figure S1) demonstrating high purities and reasonable dismutase activities of the final products.

Preparation of the Apo Form of SOD1. Dried powder of holo-SOD1 was dissolved in 50 mM sodium phosphate (pH 7.4), and then the solution pH was gradually decreased by dialysis against 50 mM sodium acetate (pH 3.8) for 6 h. Demetalation was performed by a 48 h dialysis against 50 mM sodium acetate (pH 3.8) containing 10 mM ethylenediaminetetraacetic acid (EDTA).[12] After the demetalation, EDTA was removed by dialysis against 50 mM sodium acetate (pH 3.8) supplemented with 0.1 M NaCl for 48 h.[36] Desalting and subsequent buffer exchange were performed by two successive 24 h dialyses against 50 mM sodium acetate (pH 3.8) and 50 mM sodium phosphate (pH 7.4), respectively. All the demetalation procedures described above were performed at 4 °C to minimize any thermal effects on the structure of the metal-depleted protein. The complete removal of Cu^{2+} and Zn^{2+} ions from the final sample was ensured by an analysis with a polarized Zeeman atomic absorption spectrophotometer (Hitachi Z-5010). The solution of metal-removed SOD1 (apo-SOD1) was quick-frozen in liquid nitrogen and then stored at −80 °C.

Determination of the Protein Concentration. The concentration of human SOD1 in the holo or apo form was determined by Bradford's Coomassie Brilliant Blue method using bovine SOD1 (CALZYME Laboratories) as a standard protein.[37] A literature value of the molar extinction coefficient of bovine SOD1 (ε_{258} = 10300 M^{-1} cm^{-1} in the dimeric holo form) was used to calibrate the absorption intensities at 595 nm of the protein samples stained with Coomassie dye.[12] The concentration of human SOD1 thus determined will be expressed in monomer units throughout this paper.

Acquisition of Spectral Data. CD spectra of SOD1 were recorded at room temperature (~23 °C) and pH 7.4 (50 mM phosphate buffer) on a Jasco J-820 spectropolarimeter using a quartz cell with a path length of 0.5 mm. The spectra of individual samples were averaged over four scans (each taking 3 min), and the measured ellipticity values were converted to mean residue molar ellipticity. Evaluation of the secondary structure contents from the observed CD spectra was performed by using CONTINLL in the CDPro package.[38] Visible−near-infrared

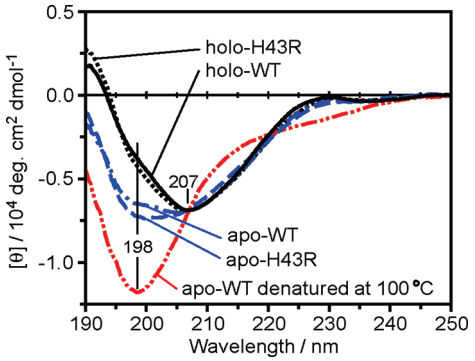

Figure 2. CD spectra of wild-type SOD1 and the H43R mutant in the holo and apo forms: holo-WT, apo-WT, holo-H43R, and apo-H43R. The spectrum of apo-WT completely denatured by heating at 100 °C for 10 min is also shown for comparison. The spectra were recorded at a protein concentration of 20 μM in 50 mM phosphate buffer (pH 7.4) using a 0.5 mm quartz cell at room temperature. The measured ellipticity values were converted to mean residue molar ellipticity. The 207 nm negative band is assigned to the β-barrel structure of the holo form and the 198 nm negative band of denatured apo-WT to irregular structure.

absorption spectra were recorded on a Hitachi U-3300 spectrophotometer using a quartz cell with a path length of 5 mm. A 3 mm × 3 mm quartz cell was used to record fluorescence spectra on a Jasco FP-6500DS spectrofluorometer.

Assay for the Pro-Oxidant Activity of SOD1. The pro-oxidant activity of apo-SOD1 was assayed by using 2′,7′-dichlorodihydrofluorescein (DCFH), which is known to be oxidized to fluorescent 2′,7′-dichlorofluorescein (DCF) by peroxidase/H_2O_2 systems and reactive oxygen species (ROS) such as $^{\bullet}OH$, $NO_2^{\bullet}$, and $CO_3^{\bullet-}$.[39−43] Fresh DCFH was prepared before use by alkaline hydrolysis of its acetylated precursor [2′,7′-dichlorodihydrofluorescein diacetate (Wako Pure Chemical Industries)].[39] The oxidation of DCFH was initiated by mixing DCFH (50 μM), H_2O_2 (50 μM), and SOD1 (10 μM in monomer units) in 50 mM phosphate buffer (pH 7.4) with or without Cu^{2+} ($CuCl_2$, 10 μM) and/or Zn^{2+} ($ZnCl_2$, 10 μM). The solution was kept in the dark for 5 min at room temperature and immediately subjected to fluorescence analysis (excitation at 495 nm, emission at 524 nm). A separate experiment using absorption spectroscopy indicated a linear increase in the amount of the oxidation product DCF over a period of more than 10 min even in the fastest reaction, indicating that the 5 min reaction time employed in the fluorometric assay is appropriate for determining the rate of DCFH oxidation. The oxidation of DCFH was also tested in the absence of H_2O_2, protein, Cu^{2+}, and/or Zn^{2+}. Autoxidation of DCFH gave a weak background fluorescence as observed for a solution of DCFH alone, and the background intensity was subtracted from the fluorescence intensity of the sample.

RESULTS

CD Spectra of Wild-Type SOD1 and the H43R Mutant. Effects of mutation on the secondary structure of SOD1 were examined by CD spectroscopy at room temperature and pH 7.4. Figure 2 shows the CD spectra of wild-type SOD1 (hereafter abbreviated as WT) and the H43R mutant in the Cu^{2+}- and Zn^{2+}-bound holo form (holo-WT and holo-H43R). Holo-WT gives a broad negative CD band mainly consisting of a strong minimum at 207 nm (black solid line in Figure 2), which is attributed to an eight-stranded antiparallel β-barrel connected by three major external loops (Figure 1).[16] The CD spectrum of holo-H43R (black dotted line) is nearly identical to that of holo-WT, indicating that the overall secondary structure is not significantly affected by the H43R mutation when the protein is properly metalated. This observation is consistent with the result of an X-ray crystallographic study of holo-SOD1 mutants including the H43R substitution.[17]

CD spectra of WT and H43R in the metal-depleted apo form (apo-WT and apo-H43R) were also examined because such metal-deficient states exist during the post-translational modifications in vivo.[7] In contrast to the holo form, the CD spectrum of the apo form exhibits an increase in negative CD intensity at 198 nm for both apo-WT (blue chain line in Figure 2) and apo-H43R (blue dashed line). To study the origin of the 198 nm negative signal, apo-WT was completely denatured by being heated at 100 °C for 10 min. The CD spectrum of the heat-denatured protein exhibits a single strong negative band at 198 nm that can be assigned to an irregular structure (red double-chain line).[44] Thus, the 198 nm negative signals in the apo-WT and apo-H43R spectra are ascribed to a partial unfolding of the polypeptide chain caused by removal of the metal. Comparison of the X-ray crystal structures of apo-WT and holo-WT has shown that the Cu^{2+} and Zn^{2+} binding sites and their neighboring loops are disordered in the apo form,[16] being consistent with the increase in negative CD at 198 nm upon removal of the metal. Apo-H43R, which shows stronger negative CD at 198 nm than apo-WT, is likely to be more disordered. Secondary structure analysis supports this interpretation (see below).

Structural Stability of Apo-SOD1. To further investigate the effect of the H43R mutation on the structural properties, apo-WT and apo-H43R were incubated at physiological temperature (37 °C) and their structures were analyzed by CD spectroscopy. Panels A and B of Figure 3 show the CD spectra of apo-WT and apo-H43R, respectively, at the 0 (no incubation), 15, 30, 45, 60, 90, and 120 min points of the 37 °C incubation. The spectrum of apo-WT does not significantly change during the incubation (Figure 3A), indicating a high conformational stability of apo-WT even at physiological temperature. In sharp contrast, apo-H43R exhibits a time-dependent growth of the negative CD signal at 198 nm, suggesting a large conformational transition involving an increase in the content of irregular structure (Figure 3B). Furthermore, two isodichroic points are observed at 208 and 220 nm for apo-H43R. Generally, the occurrence of isodichroic points is included by assuming a transition between two conformational states. In this case, the initial state of the transition must correspond to a partially disordered structure produced by the removal of active-site metal ions (hereafter called "nativelike apo form"), giving the spectrum at 0 min (before incubation) in Figure 3B. On the other hand, the final conformational state is likely to be an extensively disordered structure ("denatured apo form") because the CD spectrum of apo-H43R incubated at 37 °C for 120 min gives a strong negative CD band at 198 nm (Figure 3B), which is very similar to that of the apo-WT sample completely denatured by heating at 100 °C (Figure 2). The presence of isodichroic points indicates that the conformational transition from the nativelike apo form to the denatured apo form takes place without going through any stable intermediates. Formation of insoluble aggregates during the conformational transition is also excluded by the observation of isodichroic points.

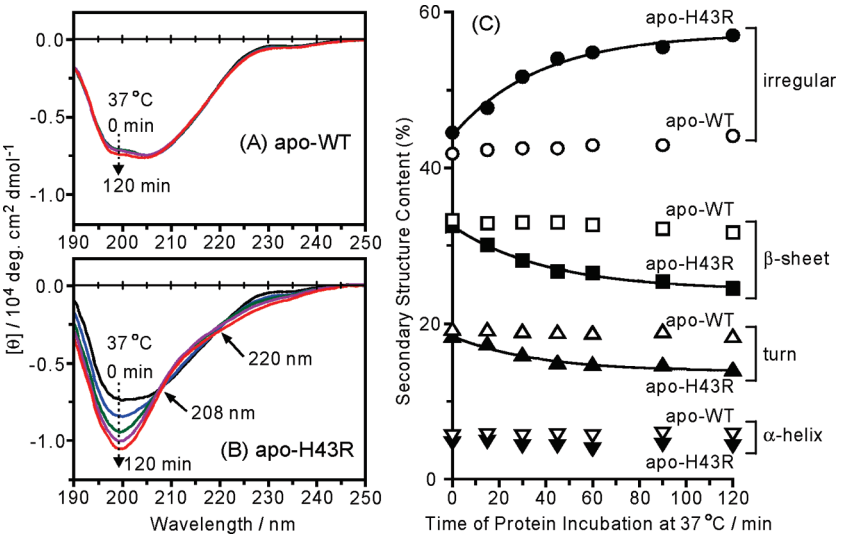

Figure 3. CD spectral and secondary structural changes during the incubation of SOD1 at 37 °C: (A) CD spectral change of apo-WT, (B) CD spectral change of apo-H43R, and (C) changes in secondary structure content calculated from the CD spectra for apo-WT (empty symbols) and apo-H43R (filled symbols). The spectra were recorded after incubation at 37 °C for 0 (no incubation), 15, 30, 45, 60, 90, and 120 min, but those at 45 and 90 min are not shown in panels A and B for the sake of clarity. Two isodichroic points at 208 and 220 nm observed for apo-H43R are indicated with arrows in panel B. Three smooth curves in panel C represent fits with exponential growth/decay functions with a common half-life of 26 min. The CD spectra were recorded at a protein concentration of 20 μM in 50 mM phosphate buffer (pH 7.4) using a 0.5 mm quartz cell at room temperature. The measured ellipticity values were converted to mean residue molar ellipticity. The secondary structure analysis was conducted with CONTINLL.

For quantitative evaluation of the structural change during the incubation at 37 °C, the secondary structure contents were calculated from the experimental CD spectra by using CONTINLL.[38] Figure 3C shows the calculated contents of α-helix, β-sheet, turn, and irregular structure as a function of the time of incubation at 37 °C. At 0 min, the content of irregular structure is slightly higher for apo-H43R than apo-WT, confirming that apo-H43R is slightly more disordered than apo-WT even before the incubation. For apo-WT (empty symbols in Figure 3C), little time dependence is seen in the secondary structure contents as expected from the CD spectra in Figure 3A. For apo-H43R, on the other hand, a large increase in the content of irregular structure and concomitant decreases in β-sheet and turn content take place during the incubation (filled symbols in Figure 3C). The time-dependent variation of the secondary structure contents of apo-H43R can be fitted to exponential growth/decay functions with a common half-life of 26 min as shown with three smooth curves in Figure 3C. This observation implies that the β-sheets and turns comprising the β-barrel decay to irregular structure following a first-order kinetics. The spontaneous and rapid decay of the β-barrel structure in apo-H43R may be ascribed to structural instability introduced by the removal of active-site metal ions. The pronounced structural instability in the apo form is a characteristic of the ALS-linked H43R mutant.

Pro-Oxidant Activity of Apo-SOD1. In addition to the structural properties of SOD1 mutants, their catalytic properties are also proposed to be relevant to the pathogenesis of ALS.[24−28] We have investigated the possible pro-oxidant activity of SOD1 by using DCFH, a fluorogenic probe for detecting pro-oxidant activity.[39−43] In a typical assay procedure, DCFH and H_2O_2 were mixed with SOD1 at room temperature, and the intensity of the green fluorescence emitted from the oxidation product DCF was recorded 5 min later to evaluate the rate of DCFH oxidation. The fluorometric DCF assay on apo-SOD1 was also conducted in the presence of Cu^{2+} and/or Zn^{2+} to examine the possibility of metal-induced pro-oxidant activity. Incubation of the protein at 37 °C prior to the fluorometric assay was adopted to investigate the effect of protein unfolding on pro-oxidant activity.

Figure 4 summarizes the DCF fluorescence intensities recorded 5 min after the various reaction components had been mixed. The column graph clearly indicates that H_2O_2 alone does not oxidize DCFH to DCF under the assay conditions used in this study (see column 1 of Figure 4). Addition of Cu^{2+} only slightly promotes the oxidation of DCFH (column 2), which is consistent with a previous report.[41] A small increase in the DCFH oxidation rate is seen in the additional presence of apo-WT (column 3) or apo-H43R (column 4), which is not incubated at 37 °C. Incubation of the protein at 37 °C for 90 min does not much affect the rate of DCFH oxidation by apo-WT (column 5) but very strongly enhances the pro-oxidant activity of apo-H43R (column 6). The high pro-oxidant activity of apo-H43R after the 37 °C incubation is largely diminished in the absence of H_2O_2 (column 7) or Cu^{2+} (column 8). No significant pro-oxidant activity is seen for holo-H43R, which contains Cu^{2+} at the native Cu-binding site (column 9). These observations suggest that the incubation at 37 °C endows apo-H43R with marked pro-oxidant potential, which is fully expressed in the presence of Cu^{2+} and H_2O_2. The pro-oxidant potential is characteristic of apo-H43R and lacking in holo-H43R.

The dependence of the pro-oxidant potential of apo-H43R on the time period of 37 °C incubation is shown in Figure 5. Seven samples of apo-H43R were individually incubated at 37 °C for 0, 15, 30, 40, 60, 90, or 120 min, and then their pro-oxidant activities were fluorometrically assayed in the presence of DCFH, H_2O_2, and Cu^{2+} (white columns). The DCF fluorescence intensity rises steeply within the first 60 min of protein incubation and then gradually increases toward a plateau over the next 60 min, indicating that the incubation at 37 °C is important for

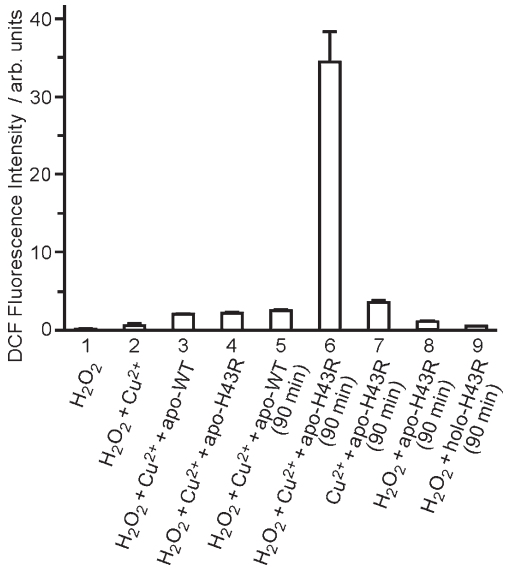

Figure 4. Intensities of fluorescence (in arbitrary units) from DCF produced by the oxidation of DCFH in the presence of (1) H_2O_2 only, (2) a mixture of H_2O_2 and Cu^{2+}, (3) H_2O_2 and Cu^{2+} mixed with apo-WT, (4) H_2O_2 and Cu^{2+} mixed with apo-H43R, (5) H_2O_2 and Cu^{2+} mixed with apo-WT preincubated at 37 °C for 90 min, (6) H_2O_2 and Cu^{2+} mixed with apo-H43R preincubated at 37 °C for 90 min, (7) a mixture of Cu^{2+} and apo-H43R preincubated at 37 °C for 90 min, (8) a mixture of H_2O_2 and apo-H43R preincubated at 37 °C for 90 min, and (9) a mixture of H_2O_2 and holo-H43R preincubated at 37 °C for 90 min. The fluorescence was excited at 495 nm and monitored at 524 nm after a 5 min reaction at room temperature. The initial concentrations of DCFH and H_2O_2 were 50 μM, and the concentrations of Cu^{2+} and proteins were 10 μM (for proteins, in monomer units). Three independent assays were conducted, and the error bars represent standard errors of the mean.

apo-H43R to acquire the pro-oxidant potential. The pro-oxidant activity of Cu^{2+}-supplemented apo-H43R is further enhanced in the additional presence of Zn^{2+} (hatched columns), though Zn^{2+} alone does not induce any significant pro-oxidant activity (black columns). The Cu^{2+} ion is essential for apo-H43R to exhibit pro-oxidant activity, and the Zn^{2+} ion assists the activity directly or indirectly.

Correlation between the Pro-Oxidant Potential and Structure of Apo-H43R. As described above, the incubation at 37 °C induces unfolding of apo-H43R and promotes the conversion from the nativelike apo form to the denatured apo form (Figure 3). Furthermore, the incubation at 37 °C endows apo-H43R with pro-oxidant potential, which increases with the time of incubation (Figure 5). To further examine the relationship between the protein structure and the pro-oxidant potential, we have plotted the DCF fluorescence intensity observed for Cu^{2+}-supplemented or Cu^{2+}- and Zn^{2+}-supplemented apo-H43R (Figure 5) against the content of irregular structure obtained from the CD spectra (Figure 3C). The plot in Figure 6 clearly indicates a strong correlation between the DCF fluorescence intensity and the content of irregular structure (correlation coefficients of 0.973 for addition of Cu^{2+} and 0.997 for addition of Cu^{2+} and Zn^{2+}). Because the DCF fluorescence intensity is a measure of pro-oxidant activity and the irregular structure content serves as a measure of the population of the denatured apo form, the strong positive correlation in Figure 6 suggests that the pro-oxidant potential arises from the denatured apo form. The denatured apo form is rich in irregular structure as shown by

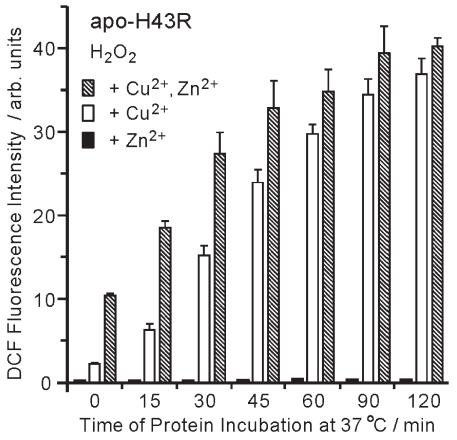

Figure 5. Dependence of the pro-oxidant activity of apo-H43R on the time of incubation at 37 °C. Samples of apo-H43R were individually incubated at 37 °C for 0, 15, 30, 45, 60, 90, or 120 min and added to a mixture of DCFH and H_2O_2 supplemented with Cu^{2+}, Zn^{2+}, or both. The initial concentrations of DCFH and H_2O_2 in the reaction mixture were 50 μM, and the concentrations of the protein, Cu^{2+}, and Zn^{2+} (if present) were 10 μM. The DCF fluorescence intensity at 524 nm was recorded after a 5 min reaction using an excitation wavelength of 495 nm. Three independent assays were conducted, and the error bars represent standard errors of the mean.

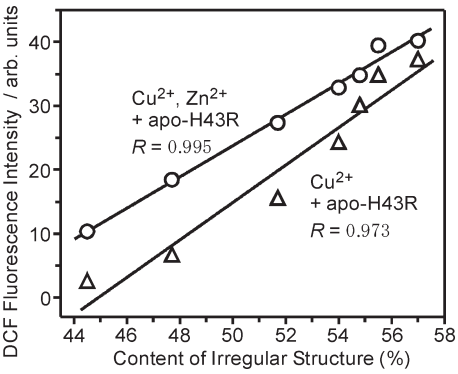

Figure 6. Correlation between the DCF fluorescence intensity in Figure 5 and the content of irregular structure in Figure 3C. The correlation coefficient was 0.973 for the DCF fluorescence data observed in the presence of Cu^{2+}. A slightly better correlation (0.995) was observed for the DCF fluorescence assays in the presence of both Cu^{2+} and Zn^{2+}. The content of irregular structure was calculated from the CD spectrum observed in the absence of metal ions.

CD spectroscopy (Figure 3), and the unfolded or misfolded polypeptide chain may provide Cu^{2+} binding sites, where the redox-active Cu^{2+} ion is activated to catalyze peroxidation and/or ROS production, leading to the oxidation of DCFH. H_2O_2 is likely to serve as an electron acceptor (oxidizing agent) in the conversion of DCFH to DCF by the activated Cu^{2+} ion. This may be the mechanism by which the denatured apo form of H43R exhibits pro-oxidant activity in the presence of Cu^{2+} and H_2O_2.

The pro-oxidant activity of apo-H43R was elevated by the co-addition of Cu^{2+} and Zn^{2+} compared to the addition of Cu^{2+} alone (Figure 5). This observation may be explained as follows. The nativelike apo form of H43R is not largely deformed from the holo form as shown by CD spectra (Figurer 2) and is

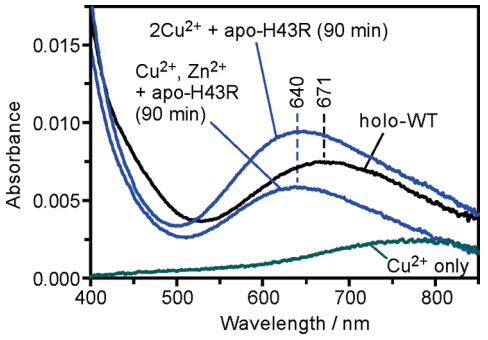

Figure 7. Visible−near-infrared absorption spectra of Cu^{2+}- and Zn^{2+}-bound holo-WT and mixtures of apo-H43R (incubated at 37 °C for 90 min) with equimolar Cu^{2+} and Zn^{2+} or 2 equiv of Cu^{2+}. The absorption bands at 671 and 640 nm are assigned to d−d transitions of the Cu^{2+} ion bound to the individual proteins. The spectrum of a solution containing Cu^{2+} alone is also shown, and the absorption around 800 nm is ascribed to a d−d transition of hydrated Cu^{2+}. Aqueous solutions of the metal ions were prepared from chloride salts. The samples were dissolved in 50 mM phosphate buffer (pH 7.4) at a concentration of 160 μM (in monomer units for SOD1 protein) and placed in a quartz cell with a path length of 5 mm.

therefore expected to be able to reversibly accommodate Cu^{2+} and Zn^{2+} in the native metal binding sites. (Such native metal binding sites may be destroyed in the denatured apo form.) Because the native Zn^{2+} site has an affinity for Cu^{2+} as well,[45] addition of Cu^{2+} alone to the nativelike apo form would induce binding of Cu^{2+} not only to the Cu^{2+} site but also to the Zn^{2+} site. Co-addition of Cu^{2+} and Zn^{2+}, on the other hand, would prevent the Cu^{2+} ion from binding to the Zn^{2+} site of the nativelike apo form, thereby increasing the number of Cu^{2+} ions available to the denatured apo form and enhancing the pro-oxidant activity of a mixture of the nativelike and denatured apo forms. This interpretation is supported by the observation that the effect of Zn^{2+} co-addition on the DCF fluorescence intensity (pro-oxidant activity) is more pronounced at lower levels of irregular structure (at higher proportions of the nativelike apo form) in Figure 6.

Interaction of Cu^{2+} with Apo-H43R. To examine the interaction of Cu^{2+} with the denatured apo form of H43R, we recorded the visible−near-infrared absorption spectra of apo-H43R (incubated at 37 °C for 90 min) in the presence of equimolar Cu^{2+} and Zn^{2+} or 2 equiv of Cu^{2+}. The spectrum of holo-WT was also recorded for comparison. As shown in Figure 7, holo-WT, containing Cu^{2+} and Zn^{2+}, exhibits an absorption at 671 nm due to a d−d transition of the Cu^{2+} ion bound to the native Cu^{2+} binding site. (The filled d orbitals of Zn^{2+} do not give rise to d−d transitions.) On the other hand, apo-H43R mixed with equimolar Cu^{2+} and Zn^{2+} shows an absorption at 640 nm, which is also ascribed to a Cu^{2+} d−d transition on the basis of its peak position and low intensity. In the presence of 2 equiv of Cu^{2+}, the 640 nm absorption is enhanced without a significant change in peak position. Because hydrated Cu^{2+} gives a d−d absorption around 800 nm as shown in Figure 7, the appearance of the 640 nm d−d absorption clearly indicates that Cu^{2+} binds to the denatured apo form of H43R. Furthermore, the significant blue shift of the peak position from 671 nm (holo-WT) to 640 nm (Cu^{2+}-bound apo-H43R) suggests that the Cu^{2+} binding mode of the denatured apo form of H43R differs from that of holo-WT because the wavelength of d−d absorption is sensitive to the coordination geometry and nature of the ligand.[46] Possibly, some amino acid side chains and/or main chain components of the denatured apo form of H43R provide non-native Cu^{2+} binding sites, where pro-oxidant activity is produced. The d−d transition wavelength (640 nm) of the Cu^{2+}-bound denatured apo form is independent of Zn^{2+} (Figure 7), indicating that the Zn^{2+} ion is not directly involved in Cu^{2+} binding. This is consistent with the indirect mechanism proposed in a previous section to explain the Zn^{2+}-induced enhancement of pro-oxidant activity (Figure 5).

DISCUSSION

In this study, we have shown that the ALS-linked H43R mutant exhibits significant structural instability in the metal-depleted apo form, and apo-H43R spontaneously unfolds or misfolds into an irregular structure at physiological temperature. The denatured apo form of H43R acquires pro-oxidant potential, which is fully expressed in the presence of Cu^{2+} and H_2O_2. The structural instability leading to the pro-oxidant activity is characteristic of apo-H43R and is lacking in holo-H43R, apo-WT, and holo-WT. Currently, structural instability and pro-oxidant activity are independently hypothesized as major toxic properties that may be acquired by ALS-linked SOD1 mutants.[20−28] Here, we have demonstrated that both toxic properties are not always mutually independent and the structural instability can lead to pro-oxidant activity.

The structural instability of apo-H43R may be related to the role of His43 in protein architecture. In the crystal structure of WT (holo-WT and apo-WT),[16,17] His43 forms a hydrogen bond with the main chain C═O group of His120 (a Cu ligand) inside the β-barrel, and the imidazole ring plane of His43 faces the side chain of Leu38, which works as a hydrophobic cork to close one end of the β-barrel. In the H43R mutant, on the other hand, the elongated side chain of Arg introduced by the mutation clashes with neighboring residues and loosens the residue packing near the hydrophobic cork.[17] An analogous defect of packing has been found near the other end of the β-barrel in another ALS-linked mutant, Ala4Val (A4V), which is also unstable compared to WT.[47] Accordingly, packing defects near the ends of the β-barrel are likely to introduce an inherent instability into the structure of mutant SOD1.

Because the active-site Cu^{2+} and Zn^{2+} ions make a contribution to the structural stability of SOD1,[13] removal of these metal ions is expected to enhance the inherent structural instability of H43R. Actually, apo-H43R readily unfolds or misfolds into an irregular structure at physiological temperature as demonstrated in this study. Thermal unfolding at physiological temperature was also reported for two other ALS-linked mutants, A4V and Gly93Ala (G93A), in the apo form if these mutants were further destabilized via cleavage of the Cys57−Cys146 intrasubunit disulfide bridge.[22] For the apo-H43R studied here, no reduction of the disulfide bridge is needed to induce denaturation at physiological temperature, suggesting that apo-H43R is more unstable than the apo forms of A4V and G93A. Structural destabilization in the apo form has also been found for ~20 other ALS-linked mutants via examination of the resistance to denaturants,[48,49] acid,[50] or heat[51,52] under varied solution conditions. Significant structural instability in the apo form appears to be a common characteristic of a number of ALS-linked SOD1 mutants, including H43R.

Binding of Cu^{2+} to the denatured apo form of H43R is a key step that the protein must take to acquire pro-oxidant activity as described in Results. Copper is a redox-active metal that can catalyze reduction and/or oxidation by recycling between the oxidized Cu^{2+} and reduced Cu^{+} forms. The redox activity of Cu in Cu-binding proteins is controlled by designed coordination of amino acid residues at the native binding sites.[53,54] In denatured proteins, however, such native Cu-binding sites are likely to be destroyed, and Cu ligand residues exposed on the protein surface would form non-native binding sites that cannot control the Cu redox activity. Probably, the denatured apo form of H43R has one or more non-native Cu^{2+} binding sites where Cu^{2+} ions are activated to catalyze peroxidation or ROS production with the help of H_2O_2. Although further details of the reaction mechanism are not clear at present, aberrant chemical reactivity of the Cu^{2+} ions bound to non-native binding sites has been implicated also in other neurodegenerative diseases.[53−55]

Several lines of evidence support the involvement of Cu^{2+} in the pathogenesis of ALS. Cu^{2+} chelators reduce the oxidative activities of ALS-linked SOD1 mutants in vitro.[24] The survival time of transgenic mice overexpressing an ALS-linked mutant of human SOD1 is extended by administration of Cu^{2+} chelators[56,57] and shortened by decreasing the level of genetic expression of metallothioneins that bind and detoxify heavy metals such as Cu^{2+}.[58] The pro-oxidant activity of the Cu^{2+}-bound denatured apo form of H43R is consistent with these observations.

In vivo, the native holo form of SOD1 is prepared by post-translational modifications of disulfide-reduced, metal-unbound immature SOD1. The copper chaperone for SOD1 (CCS) assists in the formation of the intrasubunit Cys57−Cys146 bridge and inserts Cu into the Cu-binding site.[59−62] The recognition of apo-SOD1 by CCS may be efficient for WT. However, some ALS-linked mutants in the apo form are structurally unstable, and the denatured apo form would not be properly recognized by CCS.[11,60] Nevertheless, the denatured protein may have a chance to bind Cu, which is released from CCS or supplied by CCS-independent pathways,[63] because SOD1 is abundant in motor neurons,[64] mutant SOD1 has a higher affinity for Cu than wild-type SOD1,[65] and Cu accumulates in motor neurons expressing mutant SOD1.[66]

The Cu-bound denatured apo form of mutant SOD1 exerts significant pro-oxidant activity in the presence of H_2O_2. Because the concentration of H_2O_2 in vivo ranges from 10^{-2} to 10^{2} μM,[67] it may be possible that the Cu-bound denatured SOD1 mutant encounters H_2O_2 molecules in neuronal cells and causes oxidative damage to cellular components. In fact, motor neuron-like cells expressing the ALS-linked A4V, Gly85Arg (G85R), and G93A mutants, which are all unstable in the apo form like H43R,[22,47,48] have been reported to be more susceptible to H_2O_2-induced cell death compared to the cells expressing WT.[68] A correlation between the instability of the SOD1 mutant and the rate of disease progression has also been reported.[69] The structural instability and the resultant Cu^{2+}-dependent pro-oxidant activity of mutant SOD1 may be relevant to the pathogenesis of ALS, presumably in cases with rapid disease progression such as H43R-associated ALS.

CONCLUSION

The H43R mutant of SOD1 acquires strong structural instability in the apo form and readily unfolds or misfolds into an irregular structure at physiological temperature. The denatured apo form of H43R binds Cu^{2+} at non-native binding sites and exhibits pro-oxidant activity, which is largely enhanced in the presence of H_2O_2. Because some other ALS-linked mutants of SOD1 also exhibit structural instability, the pro-oxidant activity in the presence of Cu^{2+} and H_2O_2 is likely to be shared by such mutants. Although further extensive studies are required to generalize the relationship between structural instability and pro-oxidant activity, this study raises the possibility that the Cu^{2+}-dependent pro-oxidant activity of denatured mutant SOD1 may be one of the pathogenic mechanisms of ALS.

ASSOCIATED CONTENT

Supporting Information. Experimental details for expression, isolation, purification, and characterization of recombinant SOD1 and purity and activity data of the final protein products (Figure S1). This material is available free of charge via the Internet at http://pubs.acs.org.

AUTHOR INFORMATION

Corresponding Author

*Phone and fax: +81-22-795-6855. E-mail: takeuchi@m.tohoku.ac.jp.

ACKNOWLEDGMENT

We are grateful to Prof. Takemi Enomoto and Ms. Eri Inoue of Tohoku University for a gift of a pET15b vector containing wild-type human SOD1 cDNA fused with an N-terminal hexa-His -tag and for guidance in mutagenesis and protein expression.

ABBREVIATIONS

A4V, Ala4Val mutant of human SOD1; ALS, amyotrophic lateral sclerosis; apo-H43R, apo form of H43R; apo-SOD1, apo form of human SOD1; apo-WT, apo form of WT; CCS, copper chaperone for SOD1; CD, circular dichroism; DCF, 2′,7′-dichlorofluorescein; DCFH, 2′,7′-dichlorodihydrofluorescein; EDTA, ethylenediaminetetraacetic acid; G85R, Gly85Arg mutant of human SOD1; G93A, Gly93Ala mutant of human SOD1; H43R, His43Arg mutant of human SOD1; holo-SOD1, holo form of human SOD1; holo-H43R, holo form of H43R; holo-WT, holo form of WT; IMAC, immobilized metal affinity chromatography; ROS, reactive oxygen species; SOD1, Cu,Zn-superoxide dismutase; WT, wild-type human SOD1.

REFERENCES

(1) Rowland, L. P., and Shneider, N. A. (2001) Amyotrophic lateral sclerosis. *N. Engl. J. Med. 344*, 1688–1700.

(2) Siddique, T., Pericak-Vance, M. A., Brooks, B. R., Roos, R. P., Hung, W.-Y., Antel, J. P., Munsat, T. L., Phillips, K., Warner, K., Speer, M., Bias, W. B., Siddique, N. A., and Roses, A. D. (1989) Linkage analysis in familial amyotrophic lateral sclerosis. *Neurology 39*, 919–925.

(3) Cleveland, D. W., and Rothstein, J. D. (2001) From Charcot to Lou Gehrig: Deciphering selective motor neuron death in ALS. *Nat. Rev. Neurosci. 2*, 806–819.

(4) Rosen, D. R., Siddique, T., Patterson, D., Figlewicz, D. A., Sapp, P., Hentati, A., Donaldson, D., Goto, J., O'Regan, J. P., Deng, H. X., Rahmani, Z., Krizus, A., McKenna-Yasek, D., Cayabyab, A., Gaston, S., Tanzi, R., Halperin, J. J., Herzfeldt, B., Van den Berg, R., Hung, W.-Y., Bird, T., Deng, G., Mulder, D. W., Smith, C., Laing, N. G., Soriano, E., Pericak-Vance, M. A., Haines, J., Rouleau, G. A., Gusella, J., Horvitz, H. R., and Brown, R. H., Jr. (1993) Mutations in Cu/Zn superoxide

dismutase gene are associated with familial amyotrophic lateral sclerosis. *Nature 362*, 59–62.

(5) Deng, H.-X., Hentati, A., Tainer, J. A., Iqbal, Z., Cayabyab, A., Hung, W.-Y., Getzoff, E. D., Hu, P., Herzfeldt, B., Roos, R. P., Warner, C., Deng, G., Soriano, E., Smyth, C., Parge, H. E., Ahmed, A., Roses, A. D., Hallewell, R. A., Pericak-Vance, M. A., and Siddique, T. (1993) Amyotrophic lateral sclerosis and structural defects in Cu,Zn superoxide dismutase. *Science 261*, 1047–1051.

(6) Bruijn, L. I., Miller, T. M., and Cleveland, D. W. (2004) Unraveling the mechanisms involved in motor neuron degeneration in ALS. *Annu. Rev. Neurosci. 27*, 723–749.

(7) Valentine, J. S., Doucette, P. A., and Potter, S. Z. (2005) Copper-zinc superoxide dismutase and amyotrophic lateral sclerosis. *Annu. Rev. Biochem. 74*, 563–593.

(8) Andersen, P. M. (2006) Amyotrophic lateral sclerosis associated with mutations in the CuZn superoxide dismutase gene. *Curr. Neurol. Neurosci. Rep. 6*, 37–46.

(9) Gamez, J., Corbera-Bellalta, M., Nogales, G., Raguer, N., García-Arumí, E., Badia-Canto, M., Lladó-Carbó, E., and Alvarez-Sabín, J. (2006) Mutational analysis of the Cu/Zn superoxide dismutase gene in a Catalan ALS population: Should all sporadic ALS cases also be screened for SOD1? *J. Neurol. Sci. 247*, 21–28.

(10) Rakhit, R., and Chakrabartty, A. (2006) Structure, folding, and misfolding of Cu,Zn superoxide dismutase in amyotrophic lateral sclerosis. *Biochim. Biophys. Acta 1762*, 1025–1037.

(11) Seetharaman, S. V., Prudencio, M., Karch, C., Holloway, S. P., Borchelt, D. R., and Hart, P. J. (2009) Immature copper-zinc superoxide dismutase and familial amyotrophic lateral sclerosis. *Exp. Biol. Med. (Maywood, NJ, U.S.) 234*, 1140–1154.

(12) McCord, J. M., and Fridovich, I. (1969) Superoxide dismutase. An enzymic function for erythrocuprein (hemocuprein). *J. Biol. Chem. 244*, 6049–6055.

(13) Arnesano, F., Banci, L., Bertini, I., Martinelli, M., Furukawa, Y., and O'Halloran, T. V. (2004) The unusually stable quaternary structure of human Cu,Zn-superoxide dismutase 1 is controlled by both metal occupancy and disulfide status. *J. Biol. Chem. 279*, 47998–478003.

(14) Briggs, R. G., and Fee, J. A. (1978) Further characterization of human erythrocyte superoxide dismutase. *Biochim. Biophys. Acta 537*, 86–99.

(15) Barra, D., Martini, F., Bannister, J. V., Schininà, M. E., Rotilio, G., Bannister, W. H., and Bossa, F. (1980) The complete amino acid sequence of human Cu/Zn superoxide dismutase. *FEBS Lett. 120*, 53–56.

(16) Strange, R. W., Antonyuk, S., Hough, M. A., Doucette, P. A., Rodriguez, J. A., Hart, P. J., Hayward, L. J., Valentine, J. S., and Hasnain, S. S. (2003) The structure of holo and metal-deficient wild-type human Cu,Zn superoxide dismutase and its relevance to familial amyotrophic lateral sclerosis. *J. Mol. Biol. 328*, 877–891.

(17) DiDonato, M., Craig, L., Huff, M. E., Thayer, M. M., Cardoso, R. M., Kassmann, C. J., Lo, T. P., Bruns, C. K., Powers, E. T., Kelly, J. W., Getzoff, E. D., and Tainer, J. A. (2003) ALS mutants of human superoxide dismutase form fibrous aggregates via framework destabilization. *J. Mol. Biol. 332*, 601–615.

(18) Gurney, M. E., Pu, H., Chiu, A. Y., Dal Canto, M. C., Polchow, C. Y., Alexander, D. D., Caliendo, J., Hentati, A., Kwon, Y. W., Deng, H. X., Chen, W., Zhai, P., Sufit, R. L., and Siddique, T. (1994) Motor neuron degeneration in mice that express a human Cu,Zn superoxide dismutase mutation. *Science 264*, 1772–1775.

(19) Wong, P. C., Pardo, C. A., Borchelt, D. R., Lee, M. K., Copeland, N. G., Jenkins, N. A., Sisodia, S. S., Cleveland, D. W., and Price, D. L. (1995) An adverse property of a familial ALS-linked SOD1 mutation causes motor neuron disease characterized by vacuolar degeneration of mitochondria. *Neuron 14*, 1105–1116.

(20) Bruijn, L. I., Houseweart, M. K., Kato, S., Anderson, K. L., Anderson, S. D., Ohama, E., Reaume, A. G., Scott, R. W., and Cleveland, D. W. (1998) Aggregation and motor neuron toxicity of an ALS-linked SOD1 mutant independent from wild-type SOD1. *Science 281*, 1851–1854.

(21) Stathopulos, P. B., Rumfeldt, J. A., Scholz, G. A., Irani, R. A., Frey, H. E., Hallewell, R. A., Lepock, J. R., and Meiering, E. M. (2003) Cu/Zn superoxide dismutase mutants associated with amyotrophic lateral sclerosis show enhanced formation of aggregates in vitro. *Proc. Natl. Acad. Sci. U.S.A. 100*, 7021–7026.

(22) Furukawa, Y., and O'Halloran, T. V. (2005) Amyotrophic lateral sclerosis mutations have the greatest destabilizing effect on the apo- and reduced form of SOD1, leading to unfolding and oxidative aggregation. *J. Biol. Chem. 280*, 17266–17274.

(23) Deng, H. X., Shi, Y., Furukawa, Y., Zhai, H., Fu, R., Liu, E., Gorrie, G. H., Khan, M. S., Hung, W. Y., Bigio, E. H., Lukas, T., Dal Canto, M. C., O'Halloran, T. V., and Siddique, T. (2006) Conversion to the amyotrophic lateral sclerosis phenotype is associated with intermolecular linked insoluble aggregates of SOD1 in mitochondria. *Proc. Natl. Acad. Sci. U.S.A. 103*, 7142–7147.

(24) Wiedau-Pazos, M., Goto, J. J., Rabizadeh, S., Gralla, E. B., Roe, J. A., Lee, M. K., Valentine, J. S., and Bredesen, D. E. (1996) Altered reactivity of superoxide dismutase in familial amyotrophic lateral sclerosis. *Science 271*, 515–518.

(25) Yim, M. B., Kang, J. H., Yim, H. S., Kwak, H. S., Chock, P. B., and Stadtman, E. R. (1996) A gain-of-function of an amyotrophic lateral sclerosis-associated Cu,Zn-superoxide dismutase mutant: An enhancement of free radical formation due to a decrease in Km for hydrogen peroxide. *Proc. Natl. Acad. Sci. U.S.A. 93*, 5709–5714.

(26) Ghadge, G. D., Lee, J. P., Bindokas, V. P., Jordan, J., Ma, L., Miller, R. J., and Roos, R. P. (1997) Mutant superoxide dismutase-1-linked familial amyotrophic lateral sclerosis: Molecular mechanisms of neuronal death and protection. *J. Neurosci. 17*, 8756–8766.

(27) Said Ahmed, M., Hung, W. Y., Zu, J. S., Hockberger, P., and Siddique, T. (2000) Increased reactive oxygen species in familial amyotrophic lateral sclerosis with mutations in SOD1. *J. Neurol. Sci. 176*, 88–94.

(28) Beretta, S., Sala, G., Mattavelli, L., Ceresa, C., Casciati, A., Ferri, A., Carr, M. T., and Ferrarese, C. (2003) Mitochondrial dysfunction due to mutant copper/zinc superoxide dismutase associated with amyotrophic lateral sclerosis is reversed by N-acetylcysteine. *Neurobiol. Dis. 13*, 213–221.

(29) Beck, M., Sendtner, M., and Toyka, K. V. (2007) Novel SOD1 N86K mutation is associated with a severe phenotype in familial ALS. *Muscle Nerve 36*, 111–114.

(30) Toyama, A., Takahashi, Y., and Takeuchi, H. (2004) Catalytic and structural role of a metal-free histidine residue in bovine Cu-Zn superoxide dismutase. *Biochemistry 43*, 4670–4679.

(31) Inoue, E., Tano, K., Yoshii, H., Nakamura, J., Tada, S., Watanabe, M., Seki, M., and Enomoto, T. (2010) SOD1 is essential for the viability of DT40 cells and nuclear SOD1 functions as a guardian of genomic DNA. *J. Nucleic Acids*,No. 795946.

(32) Leinweber, B., Barofsky, E., Barofsky, D. F., Ermilov, V., Nylin, K., and Beckman, J. S. (2004) Aggregation of ALS mutant superoxide dismutase expressed in *Escherichia coli*. *Free Radical Biol. Med. 36*, 911–918.

(33) Boissinot, M., Karnas, S., Lepock, J. R., Cabelli, D. E., Tainer, J. A., Getzoff, E. D., and Hallewell, R. A. (1997) Function of the Greek key connection analysed using circular permutants of superoxide dismutase. *EMBO J. 16*, 2171–2178.

(34) Crow, J. P., Sampson, J. B., Zhuang, Y., Thompson, J. A., and Beckman, J. S. (1997) Decreased zinc affinity of amyotrophic lateral sclerosis-associated superoxide dismutase mutants leads to enhanced catalysis of tyrosine nitration by peroxynitrite. *J. Neurochem. 69*, 1936–1944.

(35) Beauchamp, C., and Fridovich, I. (1971) Superoxide dismutase: Improved assays and an assay applicable to acrylamide gels. *Anal. Biochem. 44*, 276–287.

(36) Battistoni, A., Folcarelli, S., Cervoni, L., Polizio, F., Desideri, A., Giartosio, A., and Rotilio, G. (1998) Role of the dimeric structure in Cu, Zn superoxide dismutase. pH-dependent, reversible denaturation of the monomeric enzyme from *Escherichia coli*. *J. Biol. Chem. 273*, 5655–5661.

(37) Bradford, M. M. (1976) A rapid and sensitive method for the quantitation of microgram quantities of protein utilizing the principle of protein-dye binding. *Anal. Biochem. 72*, 248–254.

(38) Sreerama, N., and Woody, R. W. (2000) Estimation of protein secondary structure from circular dichroism spectra: Comparison of

CONTIN, SELCON, and CDSSTR methods with an expanded reference set. *Anal. Biochem. 287*, 252–260.

(39) Cathcart, R., Schwiers, E., and Ames, B. N. (1983) Detection of picomole levels of hydroperoxides using a fluorescent dichlorofluorescein assay. *Anal. Biochem. 134*, 111–116.

(40) Rota, C., Chignell, C. F., and Mason, R. P. (1999) Evidence for free radical formation during the oxidation of 2′,7′-dichlorofluorescin to the fluorescent dye 2′,7′-dichlorofluorescein by horseradish peroxidase: Possible implications for oxidative stress measurements. *Free Radical Biol. Med. 27*, 873–881.

(41) Zhang, H., Joseph, J., Gurney, M., Becker, D., and Kalyanaraman, B. (2002) Bicarbonate enhances peroxidase activity of Cu,Zn-superoxide dismutase. Role of carbonate anion radical and scavenging of carbonate anion radical by metalloporphyrin antioxidant enzyme mimetics. *J. Biol. Chem. 277*, 1013–1020.

(42) Wrona, M., Patel, K., and Wardman, P. (2005) Reactivity of 2′,7′-dichlorodihydrofluorescein and dihydrorhodamine 123 and their oxidized forms toward carbonate, nitrogen dioxide, and hydroxyl radicals. *Free Radical Biol. Med. 38*, 262–270.

(43) Wardman, P. (2007) Fluorescent and luminescent probes for measurement of oxidative and nitrosative species in cells and tissues: Progress, pitfalls, and prospects. *Free Radical Biol. Med. 43*, 995–1022.

(44) Brahms, S., and Brahms, J. (1980) Determination of protein secondary structure in solution by vacuum ultraviolet circular dichroism. *J. Mol. Biol. 138*, 149–178.

(45) Valentine, J. S., Pantoliano, M. W., McDonnell, P. J., Burger, A. R., and Lippard, S. J. (1979) pH-dependent migration of copper(II) to the vacant zinc-binding site of zinc-free bovine erythrocyte superoxide dismutase. *Proc. Natl. Acad. Sci. U.S.A. 76*, 4245–4549.

(46) Sigel, H., and Martin, R. B. (1982) Coordinating properties of the amide bond. Stability and structure of metal ion complexes of peptides and related ligands. *Chem. Rev. 82*, 385–426.

(47) Cardoso, R. M., Thayer, M. M., DiDonato, M., Lo, T. P., Bruns, C. K., Getzoff, E. D., and Tainer, J. A. (2002) Insights into Lou Gehrig's disease from the structure and instability of the A4V mutant of human Cu,Zn superoxide dismutase. *J. Mol. Biol. 324*, 247–256.

(48) Lindberg, M. J., Tibell, L., and Oliveberg, M. (2002) Common denominator of Cu/Zn superoxide dismutase mutants associated with amyotrophic lateral sclerosis: Decreased stability of the apo state. *Proc. Natl. Acad. Sci. U.S.A. 99*, 16607–16612.

(49) Vassall, K. A., Stathopulos, P. B., Rumfeldt, J. A., Lepock, J. R., and Meiering, E. M. (2006) Equilibrium thermodynamic analysis of amyotrophic lateral sclerosis-associated mutant apo Cu,Zn superoxide dismutases. *Biochemistry 45*, 7366–7379.

(50) Lynch, S. M., Boswell, S. A., and Colón, W. (2004) Kinetic stability of Cu/Zn superoxide dismutase is dependent on its metal ligands: Implications for ALS. *Biochemistry 43*, 16525–16531.

(51) Rodriguez, J. A., Valentine, J. S., Eggers, D. K., Roe, J. A., Tiwari, A., Brown, R. H., Jr., and Hayward, L. J. (2002) Familial amyotrophic lateral sclerosis-associated mutations decrease the thermal stability of distinctly metallated species of human copper/zinc superoxide dismutase. *J. Biol. Chem. 277*, 15932–15937.

(52) Stathopulos, P. B., Rumfeldt, J. A., Karbassi, F., Siddall, C. A., Lepock, J. R., and Meiering, E. M. (2006) Calorimetric analysis of thermodynamic stability and aggregation for apo and holo amyotrophic lateral sclerosis-associated Gly-93 mutants of superoxide dismutase. *J. Biol. Chem. 281*, 6184–6193.

(53) Bush, A. I. (2000) Metals and neuroscience. *Curr. Opin. Chem. Biol. 4*, 184–191.

(54) Gaggelli, E., Kozlowski, H., Valensin, D., and Valensin, G. (2006) Copper homeostasis and neurodegenerative disorders (Alzheimer's, prion, and Parkinson's diseases and amyotrophic lateral sclerosis). *Chem. Rev. 106*, 1995–2044.

(55) Rauk, A. (2009) The chemistry of Alzheimer's disease. *Chem. Soc. Rev. 38*, 2698–2715.

(56) Hottinger, A. F., Fine, E. G., Gurney, M. E., Zurn, A. D., and Aebischer, P. (1997) The copper chelator d-penicillamine delays onset of disease and extends survival in a transgenic mouse model of familial amyotrophic lateral sclerosis. *Eur. J. Neurosci. 9*, 1548–1551.

(57) Nagano, S., Fujii, Y., Yamamoto, T., Taniyama, M., Fukada, K., Yanagihara, T., and Sakoda, S. (2003) The efficacy of trientine or ascorbate alone compared to that of the combined treatment with these two agents in familial amyotrophic lateral sclerosis model mice. *Exp. Neurol. 179*, 176–180.

(58) Nagano, S., Satoh, M., Sumi, H., Fujimura, H., Tohyama, C., Yanagihara, T., and Sakoda, S. (2001) Reduction of metallothioneins promotes the disease expression of familial amyotrophic lateral sclerosis mice in a dose-dependent manner. *Eur. J. Neurosci. 13*, 1363–1370.

(59) Schmidt, P. J., Kunst, C., and Culotta, V. C. (2000) Copper activation of superoxide dismutase 1 (SOD1) in vivo. *J. Biol. Chem. 275*, 33771–33776.

(60) Wong, P. C., Waggoner, D., Subramaniam, J. R., Tessarollo, L., Bartnikas, T. B., Culotta, V. C., Price, D. L., Rothstein, J., and Gitlin, J. D. (2000) Copper chaperone for superoxide dismutase is essential to activate mammalian Cu/Zn superoxide. *Proc. Natl. Acad. Sci. U.S.A. 97*, 2886–2891.

(61) Brown, N. M., Torres, A. S., Doan, P. E., and O'Halloran, T. V. (2004) Oxygen and the copper chaperone CCS regulate posttranslational activation of Cu,Zn superoxide dismutase. *Proc. Natl. Acad. Sci. U.S.A. 101*, 5518–5523.

(62) Furukawa, Y., and O'Halloran, T. V. (2006) Posttranslational modifications in Cu,Zn-superoxide dismutase and mutations associated with amyotrophic lateral sclerosis. *Antioxid. Redox Signaling 8*, 847–867.

(63) Carroll, M. C., Girouard, J. B., Ulloa, J. L., Subramaniam, J. R., Wong, P. C., Valentine, J. S., and Culotta, V. C. (2004) Mechanisms for activating Cu- and Zn-containing superoxide dismutase in the absence of the CCS Cu chaperone. *Proc. Natl. Acad. Sci. U.S.A. 101*, 5964–5969.

(64) Pardo, C. A., Xu, Z., Borchelt, D. R., Price, D. L., Sisodia, S. S., and Cleveland, D. W. (1995) Superoxide dismutase is an abundant component in cell bodies, dendrites, and axons of motor neurons and in a subset of other neurons. *Proc. Natl. Acad. Sci. U.S.A. 92*, 954–958.

(65) Watanabe, S., Nagano, S., Duce, J., Kiaei, M., Li, Q. X., Tucker, S. M., Tiwari, A., Brown, R. H., Jr., Beal, M. F., Hayward, L. J., Culotta, V. C., Yoshihara, S., Sakoda, S., and Bush., A. I. (2007) Increased affinity for copper mediated by cysteine 111 in forms of mutant superoxide dismutase 1 linked to amyotrophic lateral sclerosis. *Free Radical Biol. Med. 42*, 1534–1542.

(66) Tokuda, E., Okawa, E., and Ono, S. (2009) Dysregulation of intracellular copper trafficking pathway in a mouse model of mutant copper/zinc superoxide dismutase-linked familial amyotrophic lateral sclerosis. *J. Neurochem. 111*, 181–191.

(67) Giorgio, M., Trinei, M., Migliaccio, E., and Pelicci, P. G. (2007) Hydrogen peroxide: A metabolic by-product or a common mediator of ageing signals?. *Nat. Rev. Mol. Cell Biol. 8*, 722–728.

(68) Zhang, F., and Zhu, H. (2006) Intracellular conformational alterations of mutant SOD1 and the implications for fALS-associated SOD1 mutant induced motor neuron cell death. *Biochim. Biophys. Acta 1760*, 404–414.

(69) Sato, T., Nakanishi, T., Yamamoto, Y., Andersen, P. M., Ogawa, Y., Fukada, K., Zhou, Z., Aoike, F., Sugai, F., Nagano, S., Hirata, S., Ogawa, M., Nakano, R., Ohi, T., Kato, T., Nakagawa, M., Hamasaki, T., Shimizu, A., and Sakoda, S. (2005) Rapid disease progression correlates with instability of mutant SOD1 in familial ALS. *Neurology 65*, 1954–1957.